

# SpatialBot: Precise Spatial Understanding with Vision Language Models

Wenxiao Cai<sup>1,2</sup>, Yaroslav Ponomarenko<sup>3</sup>, Jianhao Yuan<sup>4</sup>, Xiaoqi Li<sup>3</sup>,  
Wankou Yang<sup>5</sup>, Hao Dong<sup>3</sup>, Bo Zhao<sup>1\*</sup>

<sup>1</sup>BAAI <sup>2</sup>Stanford University <sup>3</sup>Peking University <sup>4</sup>University of Oxford <sup>5</sup>Southeast University

## Abstract

Vision Language Models (VLMs) have achieved impressive performance in 2D image understanding, however they are still struggling with spatial understanding which is the foundation of Embodied AI. In this paper, we propose SpatialBot for better spatial understanding by feeding both RGB and depth images. Additionally, we have constructed the SpatialQA dataset, which involves multi-level depth-related questions to train VLMs for depth understanding. Finally, we present SpatialBench to comprehensively evaluate VLMs' capabilities in spatial understanding at different levels. Extensive experiments on our spatial-understanding benchmark, general VLM benchmarks and Embodied AI tasks, demonstrate the remarkable improvements of SpatialBot trained on SpatialQA. The model, code and data are available at <https://github.com/BAAI-DCAI/SpatialBot>.

## 1. Introduction

Recently, Vision Language Models (VLMs) [4, 23, 40, 46, 59, 67] have demonstrated notable capabilities in general 2D visual understanding and reasoning, based on the vision-encoder based perception and language-model based reasoning. However, it is still challenging for VLMs to comprehend spatial information from 2D images merely, which plays a significant role in various real-world tasks [2, 16, 31, 37, 52], particularly in the application of embodied AI tasks such as navigation [12, 38, 63, 70] and manipulation [19, 42, 50, 58].

The main challenges for VLMs to have spatial understanding ability are in the following aspects: 1) Current VLMs have limited capacity in understanding depth information as they are only trained on RGB images without depth maps. Consequently, directly inputting depth maps into VLMs results in poor performance. 2) A well-designed dataset for training VLMs to understand depth is absent. The popular VLM tuning datasets do not have correspond-

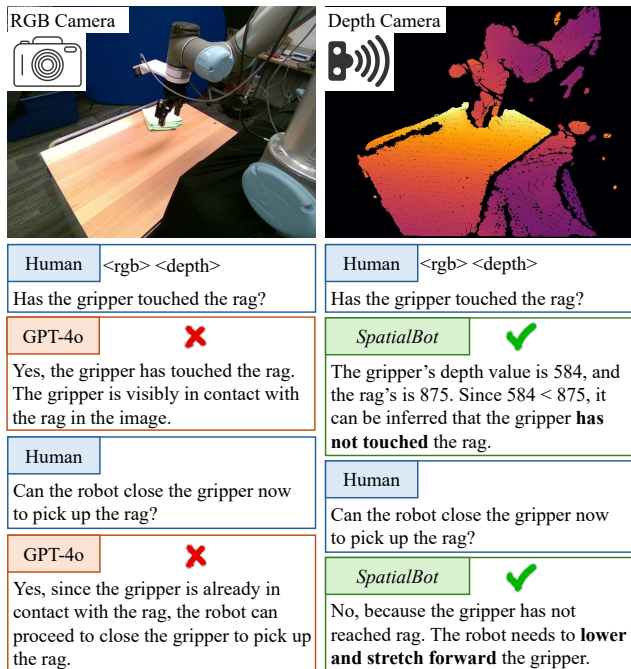


Figure 1. *SpatialBot* has better spatial understanding ability than GPT-4o. From single RGB image, even human can not judge whether the gripper has touched the rag. GPT-4o fails even if looking at both RGB and depth images. *SpatialBot* first obtains depth information of target objects from the depth map, and then judges that the gripper has not yet touched the rag.

ing depth maps, meanwhile those depth related tasks do not have question-answering-format data. 3) The inconsistency of the scales between indoor and outdoor numerical depth is also an important problem preventing VLM from uniformly processing depth in various tasks. For example, tasks such as indoor navigation and manipulation require millimeter-level precision, whereas outdoor tasks do not necessitate such high precision but demand a broader depth range.

To address these challenges, we propose *SpatialBot* that can precisely comprehend spatial information through depth images, along with the *SpatialQA* dataset for model

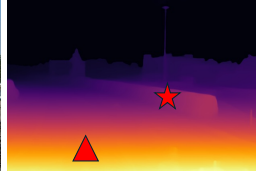
\*Corresponding author: bozhaonanjing@gmail.com

# Low-level

## Point Depth: Depth of a single point, directly retrieved from depth map

Q: What is the depth value of point (0.60, 0.58)?  
 A: point (0.60, 0.58) corresponds to a depth value of ...

Q: What is the depth value of point (0.31, 0.82)?  
 A: point (0.31, 0.82) corresponds to a depth value of ...



## Depth description and analysis

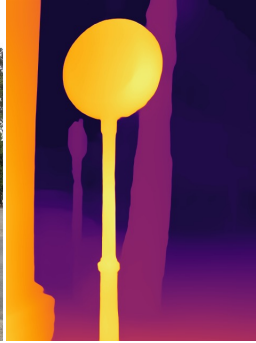
Q: Describe the depth map.  
 A: The depth map appears to depict an outdoor scene with a ground plane that extends into the distance. There are structures or objects in the middle to upper parts of the image that are further away. A vertical structure, can be seen extending upwards from the middle of the image

# Middle-level

## RGB-Depth Alignment: Depth of object, using bounding box or mask

Q: What is the metric depth of object: ROLEX clock?  
 A: The clock translates to a depth value of 4909 , with max depth 5051, min depth 4300, and mean depth 4512.

Q: How far is the pickup truck from the camera?  
 A: The pickup truck is 17802mm from the camera.



## Proximity relationships

Q: Which is closer to the camera, the ROLEX clock, or the pickup truck?  
 A: The clock has depth value of 4909, while the pickup truck corresponds to a metric depth of 17802, so the ROLEX clock is closer to the camera.

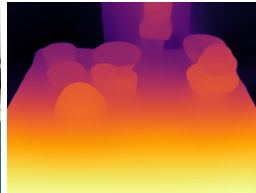
Q: Which appears to be more distant, point (0.62, 0.72) or point (0.39, 0.74)?  
 A: point (0.62, 0.72) corresponds to a depth of 3312, and point (0.39, 0.74) ...

# High-level

## Counting and enumeration

Q: How many orange bowls are there in the image?  
 A: There are 3 orange bowls.

Q: How many bowls that are upside-down are there in the image?  
 A: One.



## Spatial relationship understanding

Q: Which is closest to the gripper?  
 A: An orange bowl.

Q: If the red cup is to the right side of the gripper, what is the spatial relationship between the purple cup and gripper?  
 A: The purple cup is to the left side of gripper, and closer to the camera.

Figure 2. The proposed *SpatialQA* dataset consists of basic, middle and high level VQAs, aiming to: (a) help VLMs understand depth image, (b) let VLMs learn to align RGB and depth images, (c) enable VLMs to do high-level tasks better by understanding both RGB and depth images, as depth images provide clear boundary information and spatial relationships.

training. We source from various datasets, including general object recognition (i.e., COCO [45] and Visual Genome [35]) and robot manipulation tasks (i.e., Open X-Embodiment, or RT-X [50]), and introduce a pipeline to extend datasets from RGB to RGB-Depth through a monocular depth estimator. We design various purpose-specific QA tasks that highly rely on spatial understanding from low to high levels. These tasks include the low-level depth estimation, middle-level object detection, referring QA, and depth comparison, and high-level tasks requiring reasoning with depth such as counting, spatial relationship understanding and robot manipulation. To mitigate the problem of indoor-outdoor depth inconsistency, we design an unsigned-integral-24 (uint24) format for numerical depth representation that can preserve the raw depth values and have a broad range of values from 1mm to 131m, in millimeters. To enable the model to accurately obtain depth information, we designed a depth API that allows the model to query the depth values of individual pixels or regions by calling the API.

We validate the capacity of spatial comprehension of

VLMs with *SpatialBench* which consists of manually annotated question-answer pairs about spatial understanding and reasoning. The experimental results verify that our *SpatialBot* can better understand the depth in the three levels. Additionally, it is also verified that tuning VLMs on *SpatialQA* can improve their performances on general VLM benchmarks such as MME [17], GQA [26], etc. Finally, we perform robot manipulation tasks in RT-X to demonstrate the promising applications of *SpatialBot*. In summary, the main contributions of our work are as follows:

- We propose *SpatialBot* that shows promising performance in general visual recognition, spatial understanding, and robot manipulation. Especially, *SpatialBot* outperforms GPT-4o [67] in several depth-understanding related tasks.
- We curate a large-scale language-aligned RGB-D question answering dataset, *SpatialQA* for training *SpatialBot* and *SpatialBench* for evaluating VLMs' spatial understanding performances. Three levels of tasks have been designed for comprehensive analysis.

## 2. Related work

### 2.1. VLM and RGB datasets

In recent years, VLMs (or Multi-modal Large Language Models, MLLMs) have achieved significant advancements [30]. LLaVA [46] pioneered the visual instruction tuning, which is followed by subsequent works [4, 23, 44, 49, 69] with more extensive datasets [76] and different Large Language Models (LLM) backbones [1, 3, 10, 60]. These VLMs primarily tackle tasks related to perception [17], reasoning [48] and OCR [39, 72]. Additionally, some works have introduced an encoder-decoder structure beyond VLMs to perform pixel-level grounding tasks [36, 65, 68, 71, 74, 75]. However, their performances in counting and enumeration [14, 25] and spatial relationship understanding [28] are mediocre. We posit that comprehending the entire space from a monocular RGB image is overwhelming for VLMs. Integrating depth information could effectively enhance the spatial understanding capabilities of VLMs.

### 2.2. Spatial Understanding

Spatial understanding requires VLMs to comprehend scenes beyond 2D RGB images. This is particularly crucial in precision tasks such as robotic grasping [13]. Spatial understanding can be achieved through point clouds [13, 64] or depth maps [28]. Some studies have attempted to perform depth estimation [41] and 3D detection [11] directly from monocular RGB images, but the accuracy is limited when it comes to metric depth estimation. SpatialVLM [7] infers spatial relationships from 2D images only. However, in robotic tasks (e.g. Fig. 1), depth from sensors is a must in spatial understanding. Recently, Monocular Depth Estimation (MDE) has seen rapid advancements. By utilizing large amounts of unsupervised data [5, 66] and synthetic data [32], MDE can accurately estimate depth in various scenarios [54]. Therefore, we enhance the spatial understanding of VLMs by adding depth information to the RGB images they use, leveraging MDE. Despite the strength of monocular depth estimation models, training large models to estimate depth directly is not always feasible. In embodied AI scenarios, precise depth information is required from hardware devices, which depth estimation models cannot achieve. Additionally, enabling VLMs to precisely understand space from a single RGB image has proven to be exceedingly difficult [11, 41].

## 3. SpatialBot

We use depth information to guide VLMs in understanding space [27, 51], because compared to point clouds, depth information is easier to collect and process. Since the RGB-D cameras are cheap, most of robots carry such cameras to capture RGB and depth images instantly. In addition, due

to remarkable capacities of Monocular Depth Estimation (MDE), one can adapt large scale RGB datasets to RGB-D dataset in a fast and affordable way. Thus, we introduce depth images for spatial understanding and construct *SpatialQA* dataset with RGB-D images and depth-related QA pairs. In this section, we elaborate on the pipeline of dataset construction: collecting RGB and depth images, estimating depth images from RGB images using MDE, unifying the format of depth images, generating basic VQAs for VLM training, and generating depth related VQAs. This pipeline can be easily scaled up to construct larger datasets from available RGB datasets.

### 3.1. Depth Map Encoding

Our depth encoding aims to preserve all depth information for VLMs to use. A challenge is the indoor and outdoor consistency. Indoor scenes like robot manipulation [50] and indoor navigation [6, 22] may require millimeter-level precision, while outdoor scenes include a large range of depth values. Existing methods often adopt ordinal encoding [18, 66], which, however, cannot be subjected to basic mathematical operations. To address the issue, we use uint24 or three-channel uint8 to store depth values, measured in millimeters from  $1mm$  to  $131.071m$ . We directly save the raw depth values and leave subsequent computations to the powerful fitting capabilities of VLMs. For single-channel uint24, we use millimeter as unit directly. This way, VLMs can directly query the required values from the depth map. For three-channel uint8 images, we distribute the values across a broader range: the units for the three channels are  $2^0$ ,  $2^5$ , and  $2^{10}$  millimeters, respectively. Each channel has  $2^5$ ,  $2^5$ , and  $2^7$  possible values. For an image of size  $(H, W)$ , to store depth value  $d_{H,W}$  (in millimeters) in three-channel uint8 image  $I_{H,W}^3$ , we encode the image  $I$  following:

$$I_{h,w}^0 = (d_{h,w} / 2^{10}) * 2^1, \quad (1)$$

$$I_{h,w}^1 = (d_{h,w} / 2^5) * 2^3, \quad (2)$$

$$I_{h,w}^2 = (d_{h,w} \% 2^5) * 2^3. \quad (3)$$

The choice of  $2^{10}$  mm as a unit for the first channel is influenced by the depth range in many desktop grasping tasks in robotics [8, 15, 29, 33, 57, 61, 62], which typically have a maximum depth of around  $1m$ . A larger unit would result in the first channel being predominantly zero in most scenarios. Similarly, we use multipliers of 2 and 8 to ensure the better distinction between three-channel depth map. We believe VLMs can easily learn the relationship between our encoding method and the actual depth values, and our experiments have validated this.

If the raw data includes depth estimated by sensors, we use the raw depth values. Otherwise, for MDE, we use the ZoeDepth [5] model for estimation, as it considers both

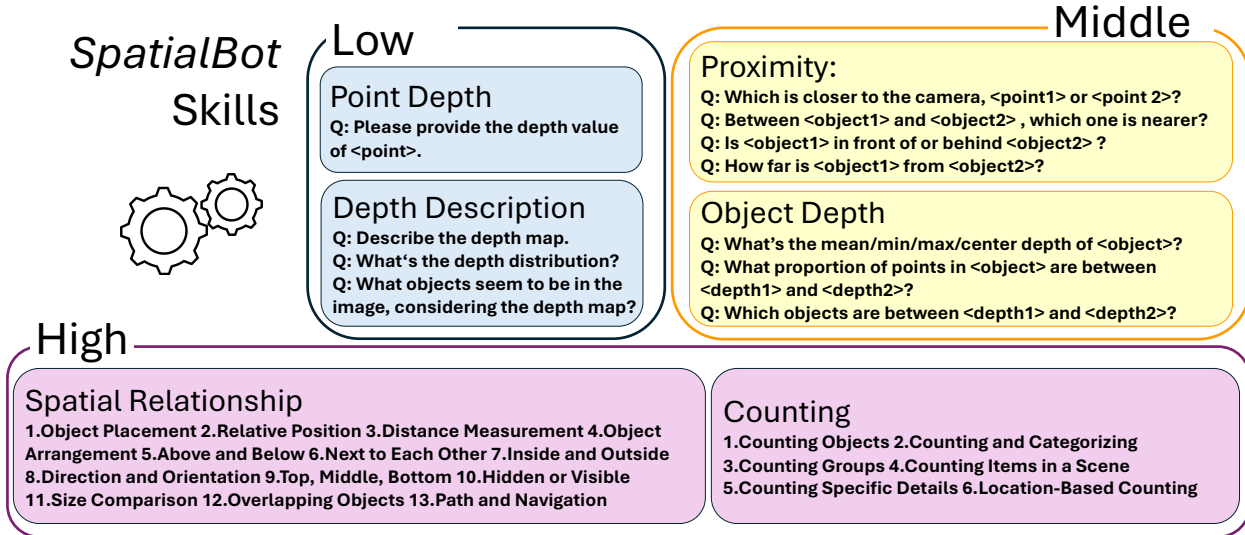


Figure 3. *SpatialBot* masters three levels of skills: (a) understanding depth images (b) aligning these RGB and depth inputs, and performing proximity comparison, (c) applying RGB-D for spatial relationship understanding and counting.

indoor and outdoor scenarios and can accurately estimate metric depth in these situations. Note that we do not use the relative depth models, such as MiDaS [54]. It is incorrect to directly take the inverse of the relative depth  $d_r$  as the actual depth  $d$ . Suppose that the maximum and minimum depth in an image is  $d_{max}$  and  $d_{min}$ , the conversion should follow:

$$A = \frac{1}{d_{min}} - \frac{1}{d_{max}}, \quad (4)$$

$$B = \frac{1}{d_{max}}, \quad (5)$$

$$d = \frac{1}{(A * d_r + B)}. \quad (6)$$

It is incorrect to ask for the depth value but uses  $\frac{1}{d_r}$  as the label in QAs [41]. While  $\frac{1}{d_r}$  can reflect the relative size of depth, it does not maintain proportional relationships (e.g.  $\frac{1}{d_r} = 0.4$  is not twice the depth of 0.2). Only when the max depth is infinite can  $\frac{1}{d_r}$  be considered as true depth multiplies by a scale factor.

### 3.2. Depth Description of an Object

*SpatialQA* is a VQA dataset, and our model is a standard VLM (Fig. 4): it takes images and text as input and outputs text. To maintain generality, we do not use a separate image encoder, so *SpatialBot* cannot output pixel-level information. Intuitively, the center point of objects can simply represent their depth. However, for example, in the case of a cup, there is a significant difference between the depth of the inner and outer surfaces, so a single value cannot accurately represent the depth. Therefore, we use four depth

values—max, min, mean, and center—to describe the object’s depth, if its mask is available. Considering that the mask and depth map cannot be perfectly precise, we use the 95th and 5th percentile values as the max and min depth values. Bounding boxes in Visual Genome (VG) [35] are very inaccurate, and our experiments find that prompting SAM [34] with these bounding boxes will yield undesirable masks. In this case, to prevent incorrect depth from misleading the model, we fall back to using only the depth of the center point of the bounding box to describe depth.

### 3.3. Image Sources

A RGB-D VLM dataset should include detailed QAs that help VLMs to understand the image, which may include reasoning, conversation, description and referring [76]. Specific object descriptions are required, e.g. in Fig. 4, woman is not a good description, but the woman in the middle or the woman standing tallest are good descriptions. Existing captioning, grounding and segmentation models [9, 47, 55, 77] can not generate detailed and specific descriptions. To this end, we base *SpatialQA* mainly on VLM data where detailed QAs are included [23].

In *SpatialQA*, we primarily include three data sources: COCO [45], VG [35], and Open X-Embodiment (RTX) [50]. Therefore, we base our dataset on Bunny\_695k [23], which includes COCO and VG. Bunny\_695k contains image QA covering reasoning, detailed descriptions, grounding, etc. On this basis, we added depth-related QA pairs. In Bunny\_695k, the bounding boxes for COCO images come from VG annotations on COCO images. We find that they are inaccurate. Since

LLaVA [46] might include some in-house data, we found that its bounding boxes predictions on COCO align well with human understanding and have much higher accuracy than publicly available ground truth and the results from other models such as GPT-4V [67], Gemini [59], Qwen-VL [4], and Bunny [23]. Therefore, we use LLaVA to refine bounding boxes and use these bounding boxes and their center points to prompt Segment Anything Model (SAM) [34] to get masks. We ensure that SAM masks do not exceed the bounding box limits, then select the mask with the highest confidence. For VG images, the bounding boxes cover only rough areas and are very inaccurate. We have not found a model with particularly good bounding box capabilities on VG. Therefore, we only use VG’s bounding boxes and the depth of the center point. RT-X integrates many robotics datasets. For datasets containing sensor depth data, we directly use the raw depth. For other datasets, we use model-estimated metric depth. We select 7.5k of these and manually annotated the bounding boxes, querying the depth information of the objects. For the remaining images, we only ask about the depth of certain pixels in the image. Also, we use GPT-4o to generate conversations based on RTX-7.5k, where we prompt GPT-4o to focus on: what robot are doing, how should the robot finish robot task, object count, object position, positional relationships and object appearance. In future versions of *SpatialQA*, we will include more images from a vast range of sources.

### 3.4. *SpatialQA* Pipeline

To help VLMs understand depth inputs, and use depth information to do high-level tasks like spatial relationship understanding, counting and enumeration, we design a three-step QA pipeline. We aim to make this pipeline effective and easy-to-follow: (a) This pipeline progressively let VLM learn to understand depth, align depth and RGB, and use depth for complex reasoning in high-level tasks. (b) existing RGB datasets can be easily converted to RGB-Depth datasets with our pipeline. *SpatialQA* pipeline is shown in Fig. 5, and the skills to learn are shown in Fig. 3.

**Low level.** To enable VLMs to understand depth images and learn to query information from them, we ask depth value of points. VLMs should learn to take the depth value directly from depth inputs, and relate point coordinates with pixels in image. In the meanwhile, since the visual encoder does not see depth images in pre-training, we also expect the encoder and projector to learn to encode depth images together with RGB images. We also let *SpatialBot* describe the depth map and infer what may be in the images, giving only a depth map.

**Middle level.** As VLMs have learnt to encode and query information from depth images, they should now learn to use depth information. Also, since image and depth inputs

are given to VLMs, they should also know the relationships between them. First, we ask about proximity relationships, namely which point is closer or further away. Second, we let VLMs learn to describe the depth of objects or regions, by using center point depth, minimum, maximum and mean depth. VLMs should learn to locate an object in the RGB image and then find depth information from depth input. Third, we ask about proximity relationships between objects.

**High level.** Since VLMs can now understand depth input, align depth with RGB and have some knowledge about proximity relationships in the spatial world, we design tasks to help VLMs apply depth at a higher level. When the model sees the depth map, the boundaries of objects and their surroundings become clearer, so we believe that the depth map aids in grounding and counting tasks. Additionally, in *SpatialQA*, the model gains a clear understanding of the space, which helps the model determine spatial and positional relationships.

### 3.5. *SpatialBench*

To evaluate VLM’s performance on high-level tasks, we annotate the *SpatialBench*. On 120 images, we ask following questions:

- Has [Object 1] touched/reached [Object 2]?
- What is the spatial relationship between [Object]s?
- Counting and enumeration.
- Size comparison between objects.

All question are in Yes/No or multiple choice formats. Additionally, *SpatialBench* includes depth and proximity questions on images from MME [17] dataset, and our manually annotated 80 images (3 bounding box per image).

### 3.6. *SpatialBot* Architecture

*SpatialBot* uses a VLM structure: Images are processed through an image encoder and a multi-modal projector, converted into tokens, and then sent along with text tokens into an LLM, which ultimately outputs responses. To enable the model to accurately obtain depth information, we designed **Depth API**. When the *SpatialBot*’s output contains text with a format of Depth(point), the API will query the depth value of that point in the corresponding depth map and then input this depth value back into *SpatialBot*. Combining the user’s question with the API’s return value, *SpatialBot* will provide the final answer. The model can call the API to get the precise depth value of a specific point. For example, when *SpatialBot* wants to know the depth information of an object, it first determines the bounding box of the object and then calls the Depth API using the center point of the bounding box. If the model wants to obtain the depth range of this object, it first observes which points in the image correspond to the maximum and minimum depth values and calls the Depth API using the coordinates of these

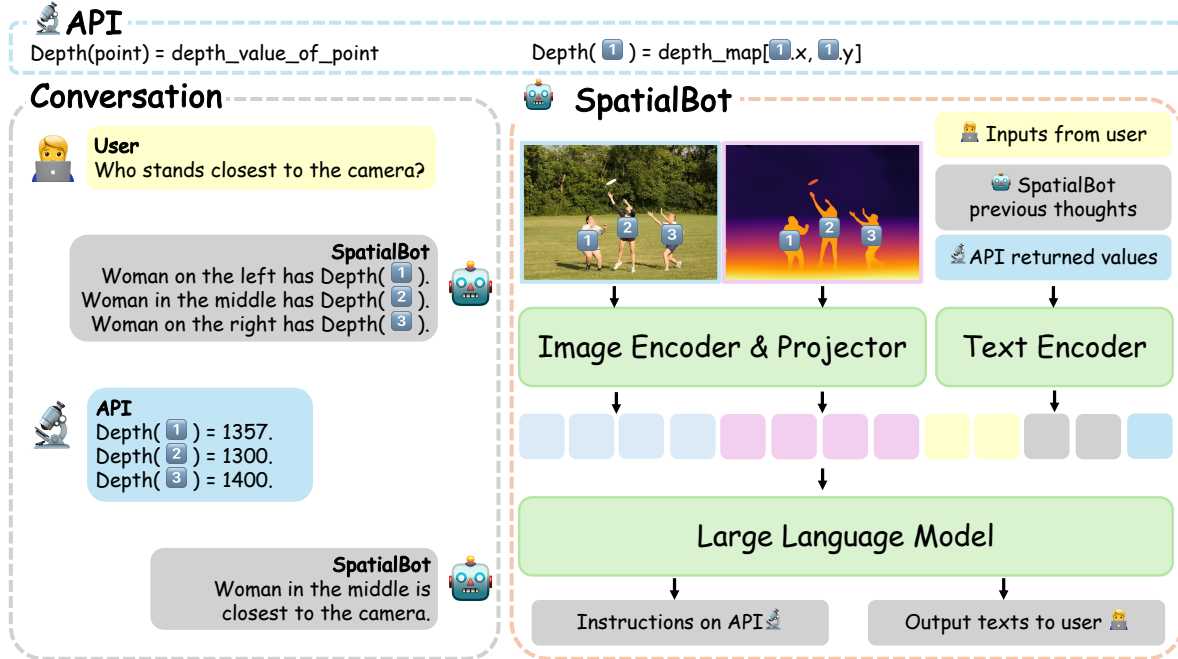


Figure 4. The architecture of *SpatialBot*. It takes a pair of RGB and depth images as input, where depth images are optional. *SpatialBot* can choose to call Depth API if it need accurate depth information.

points. However, to enhance the model’s understanding of the depth map itself, during training, we only allow *SpatialBot* to call the API on a subset of the data. For the remaining data, the model must directly use the depth map to answer the depth of the object.

## 4. Experiments

We start with validating *SpatialBot* has the ability to understand depth, extract information from depth maps, and perform high-level tasks. Then, we observe performance improvements in general VQA tasks, such as MME [17] and GQA [26], by introducing depth maps. This indicates that training on *SpatialQA* can help VLMs perform better on general tasks. Finally, experiments on RT-X [50] show that *SpatialBot* benefits from understanding depth in robot manipulation tasks.

**Implementation.** We design *SpatialBot* based on Bunny [23], a family of VLMs. Phi-2-3B, Phi-3-4B [1], QWen-1.5-4B [3] and Llama-3-8B [60] are used as the base LLM. *SpatialBot* model architecture is shown in Fig. 4. The image encoder is SigLIP [73] with 384x384 image resolution. QWen-1.5-0.5B and CLIP [53] with 336x336 image resolution are adopted in robot manipulation tasks. We pre-train models on two million image-text pairs from LAION-2B [56] (Bunny-pretrain-LAION-2M [23]) and finetune them on Bunny\_695k [23]. The learning rate is kept  $2e - 4$ , and learning rate for multi-modal projector is  $2e - 5$ , ex-

cept for Llama-3-8B, where we halve both learning rates. For manipulation tasks, we also halve the learning rate. The multi-modal projector is trainable in both pretrain and finetune stage, and we add a LoRA [24] module in finetuning. We use 8 A100 for training. On *SpatialQA*, it takes about 15 hours for Phi-2 [1].

### 4.1. Spatial Understanding

We first validate that *SpatialBot* can get accurate metric depth value from depth images or Depth API, and decide proximity relationships, which are low-level and middle level tasks in *SpatialQA*. We use bounding box and metric depth from *SpatialBench*. We then ask about depth of random points and objects in them. We tell VLMs the names w/ and w/o bounding boxes of target object. For ground truth depth value  $d_{gt}$ , estimated depth value  $d_{est}$  from VLMs, we estimate depth accuracy by  $\frac{d_{gt}-d_{est}}{d_{gt}} * 100\%$ . Results by answering with Depth API are shown in Depth and Proximity column in Table. 1. Also, we ask the proximity relationships. Sample conversations on depth map understanding and high-level tasks are shown in Fig. 7.

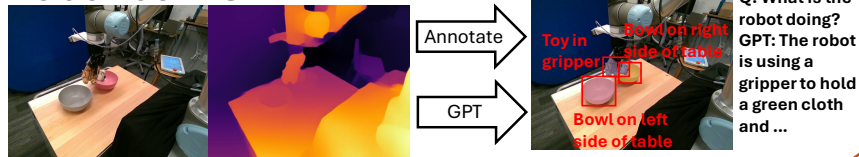
### 4.2. SpatialBench

We compare model performance on our *SpatialBench*, which composes on positional relationship, object existence, reaching and size comparison tasks. GPT-4o and LLaVA-v1.6-34B [46] without training on *SpatialQA* are

Depth  
Sensor  
Data



### Robotics-RGBD



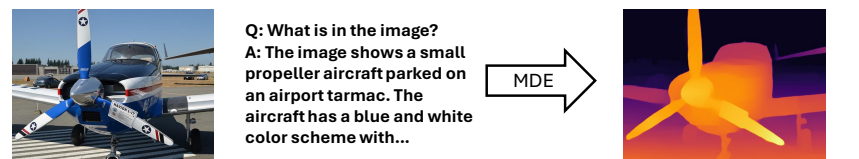
### CV-Depth



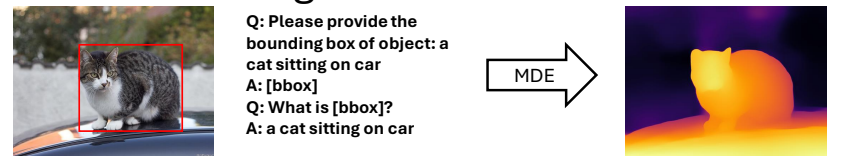
RGB  
Camera  
Data



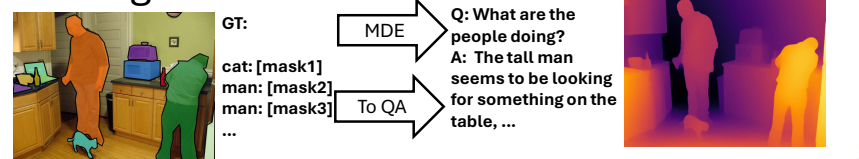
### MLLM-General



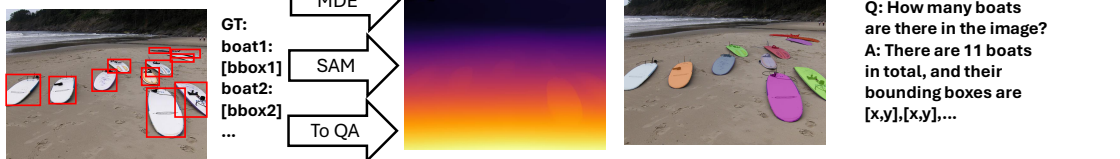
### MLLM-Referring



### CV-Segmentation



### CV-Detection



### Robotics-RGB



Figure 5. Image sources and RGB to RGB-Depth dataset conversion pipeline. RGB and depth information, captions or conversations about the images, bounding boxes or masks, and corresponding detailed descriptions of objects are required to make *SpatialQA* dataset.

Table 1. Results on *SpatialBench*. Best results of models with the same base LLMs are marked with **bold** text. LLM-*RGB* and LLM-*RGBD* are trained on RGB images only and tested with RGB and RGBD inputs, respectively. LLM-*Spatial* is trained on *SpatialQA*. For Depth and Proximity, we report results w/o calling Depth API. Every *SpatialBot* variant w/ Depth API reaches 99%+ accuracy on Depth and Proximity.

Model	Depth $\uparrow$	Proximity $\uparrow$	Position $\uparrow$	Existence $\uparrow$	Counting $\uparrow$	Reaching $\uparrow$	Size $\uparrow$
GPT-4o- <i>RGB</i>	-	39.33	70	87.5	84.45	52.00	36.67
GPT-4o- <i>RGBD</i>	-	38.00	55	82.5	85.16	51.67	35.00
Phi-2-3B- <i>RGB</i>	-	27.67	45	65.0	81.60	38.33	26.67
Phi-2-3B- <i>RGBD</i>	-	36.00	50	67.5	84.50	38.67	28.00
Phi-2-3B- <i>Spatial</i>	93.27	<b>91.30</b>	<b>50</b>	<b>72.5</b>	<b>89.93</b>	<b>41.67</b>	<b>30.00</b>
Phi-3-4B- <i>RGB</i>	-	19.67	<b>60</b>	75.0	90.56	36.67	20.00
Phi-3-4B- <i>RGBD</i>	-	22.33	45	<b>77.5</b>	91.70	39.00	18.33
Phi-3-4B- <i>Spatial</i>	94.27	<b>77.00</b>	<b>60</b>	75	<b>94.20</b>	<b>42.00</b>	<b>30.00</b>
QWen-1.5-4B- <i>RGB</i>	-	28.00	50	67.5	82.00	33.33	<b>21.67</b>
QWen-1.5-4B- <i>RGBD</i>	-	31.00	65	65.0	83.07	35.67	21.33
QWen-1.5-4B- <i>Spatial</i>	95.26	<b>79.00</b>	<b>75</b>	<b>77.5</b>	<b>94.20</b>	<b>43.33</b>	20.00
Llama-3-8B- <i>RGB</i>	-	29.33	60	75.0	90.16	43.33	16.67
Llama-3-8B- <i>RGBD</i>	-	30.67	55	70.0	82.32	45.00	20.00
Llama-3-8B- <i>Spatial</i>	93.41	<b>88.67</b>	<b>65</b>	<b>80.0</b>	<b>90.45</b>	<b>51.67</b>	<b>21.67</b>

Table 2. Results on general VLM Benchmarks. For same base LLM models, better results are marked with **bold** text. RGB-D inputs are only used in MME and GQA. We report results of model trained with RGB and tested with RGB or RGB-D in these benchmarks, split with slash.

Model	MME <sup>P</sup> $\uparrow$	MME <sup>C</sup> $\uparrow$	MMB <sup>T</sup> $\uparrow$	MMB <sup>D</sup> $\uparrow$	SEED(-I) $\uparrow$	VQA <sup>v2</sup> $\uparrow$	GQA $\uparrow$	POPE $\uparrow$
Phi-2-3B	1472/1474	286/285	67.90	<b>68.90</b>	69.91	78.98	61.52/57.93	86.21
Phi-2-3B- <i>Spatial</i>	<b>1490</b>	<b>295</b>	<b>67.94</b>	68.21	<b>70.48</b>	<b>79.84</b>	<b>62.25</b>	<b>86.60</b>
Phi-3-4B	1417/1364	308/319	70.15	70.74	71.04	<b>80.57</b>	61.18/59.97	84.60
Phi-3-4B- <i>Spatial</i>	<b>1458</b>	<b>339</b>	<b>71.30</b>	<b>71.22</b>	<b>71.63</b>	80.00	<b>62.15</b>	<b>85.13</b>
QWen-1.5-4B	1340/1364	251/254	<b>69.56</b>	<b>68.56</b>	62.38	<b>80.63</b>	62.55/62.47	85.70
QWen-1.5-4B- <i>Spatial</i>	<b>1376</b>	<b>261</b>	68.11	67.61	<b>70.44</b>	80.44	<b>63.18</b>	<b>86.12</b>
Llama-3-8B	<b>1574/1542</b>	<b>342/318</b>	73.67	74.65	72.32	80.50	63.18/62.79	85.22
LLama-3-8B- <i>Spatial</i>	1551	327	<b>74.89</b>	<b>75.43</b>	<b>72.84</b>	<b>80.95</b>	<b>63.29</b>	<b>85.74</b>

compared with models trained on *SpatialQA*. 3B, 4B and 8B models trained on *SpatialQA* reaches comparable results with GPT-4o. Results are reported in Table 1.

### 4.3. General VLM Benchmarks

We report results on general benchmarks: MME perception [17] (MME<sup>P</sup>), MME cognition (MME<sup>C</sup>), MM-Bench [48] test and dev set (MMB<sup>T</sup> and MMB<sup>D</sup>), SEED Bench Image [39] (SEED(-I)), VQA [20] test-dev split (VQA<sup>v2</sup>), GQA [26], and POPE [43] (the averaged F1-score of three categories on the validation set of COCO). In most of these benchmarks, RGB information along is enough. We only use RGB-Depth input on MME<sup>P</sup> and GQA since they contain counting, existence and position

questions, where we expect depth information can benefit such cases.

### 4.4. RT-X Robot Manipulation

We test performance of VLMs with and without depth input. Robot manipulations tasks are specified as: in current time stamp  $t$ , given history and current image observations  $x_{j=0}^t$  (with optional depth maps), models should learn policy  $\pi(i, x_{j=0}^t)$ . Action  $a_t$  is sampled from  $\pi$  and applied to robots. For a robot of two-finger end effector, action space can be  $(\Delta X, \Delta Y, \Delta Z, \Delta R, \Delta P, \Delta Y_a, C, T)$ , indicating delta change in poses  $XYZ$  and rotation  $RPY_a$  (roll, pitch, yall), gripper closure  $C$  and whether to termi-



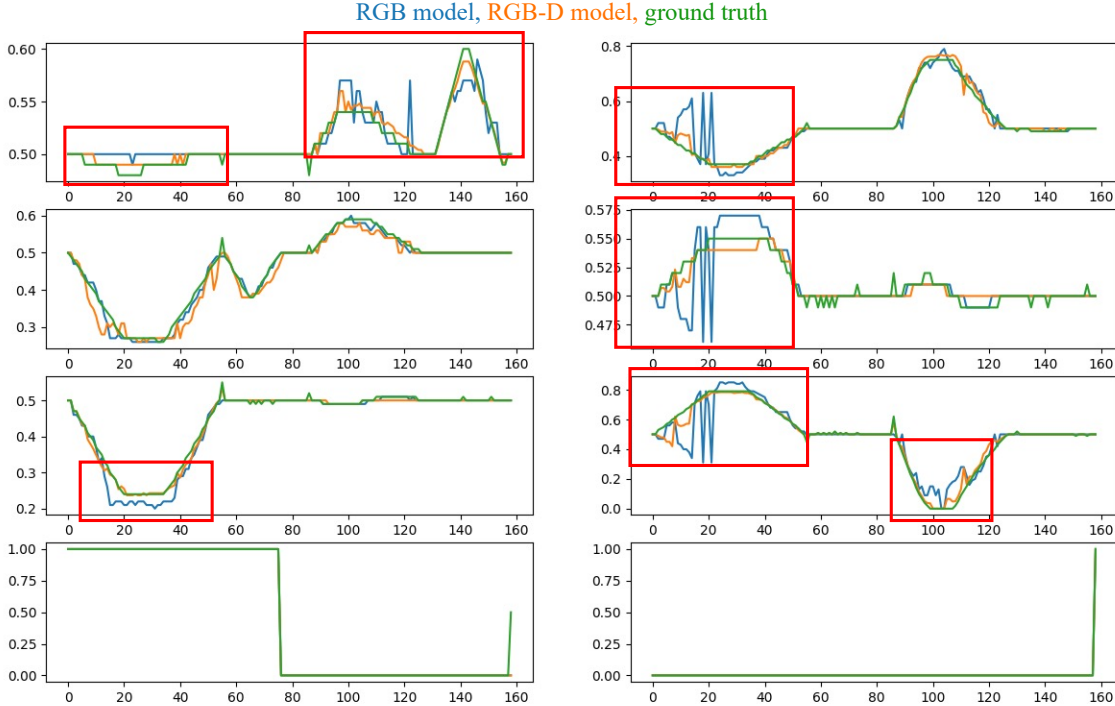


Figure 6. Results on Maniskill episode 28000. By understanding depth, models can predict robot action better. From left to right, top to bottom:  $(\Delta X, \Delta Y, \Delta Z, \Delta R, \Delta P, \Delta Y_a, C, T)$ . x-axis:  $t$ , y-axis: encoded control signal.

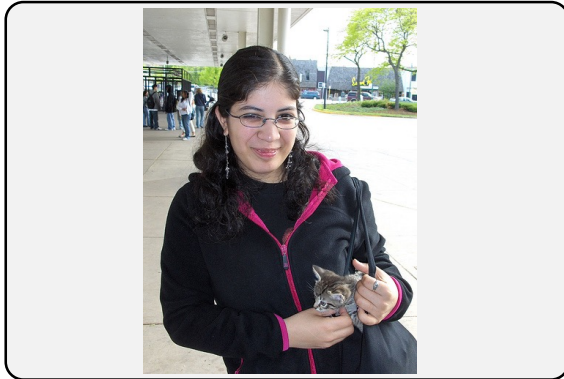
nate action  $T$ . The delta change in position and rotation of action space is encoded into 101 possible values, from 0, 0.01 to 1. We use Qwen-1.5-0.5B [3] as the base LLM, and CLIP [53] are vision encoder. The pretrain dataset is Bunny-pretrain-LAION-2M, and Maniskill data are used in finetuning. A history of 4 frames are used to predict end-effector delta pose of the current frame. We use Maniskill [21] to evaluate model performance. 7000 episodes are used in training. A sample open-loop control comparison is shown in Fig.6. By understanding depth images, *SpatialBot* can predict robot actions better.

## 5. Conclusion

We propose *SpatialQA* dataset and *SpatialBench* benchmark to train and evaluate *SpatialBot*, a family of state-of-the-art VLMs with real world space knowledge and accurate understanding of depth images. We design QAs to let VLM first query depth information from depth maps, and then use it to compare proximity relationships of points or objects. We then design high level tasks where depth information may help. Experimental results on our benchmark, general VLM benchmarks, and robot manipulation tasks show that *SpatialBot* can effectively understand and utilize depth information.

## References

- [1] Marah Abdin, Sam Ade Jacobs, Ammar Ahmad Awan, Jyoti Aneja, Ahmed Awadallah, Hany Awadalla, Nguyen Bach, Amit Bahree, Arash Bakhtiari, Harkirat Behl, et al. Phi-3 technical report: A highly capable language model locally on your phone. *arXiv preprint arXiv:2404.14219*, 2024. 3, 6
- [2] Daichi Azuma, Taiki Miyanishi, Shuhei Kurita, and Motoaki Kawanabe. Scanqa: 3d question answering for spatial scene understanding. *2022 IEEE/CVF Conference on Computer Vision and Pattern Recognition (CVPR)*, pages 19107–19117, 2021. 1
- [3] Jinze Bai, Shuai Bai, Yunfei Chu, Zeyu Cui, Kai Dang, Xiaodong Deng, Yang Fan, Wenbin Ge, Yu Han, Fei Huang, et al. Qwen technical report. *arXiv preprint arXiv:2309.16609*, 2023. 3, 6, 9
- [4] Jinze Bai, Shuai Bai, Shusheng Yang, Shijie Wang, Sinan Tan, Peng Wang, Junyang Lin, Chang Zhou, and Jingren Zhou. Qwen-vl: A versatile vision-language model for understanding, localization, text reading, and beyond. 2023. 1, 3, 5
- [5] S. Bhat, Reiner Birkel, Diana Wofk, Peter Wonka, and Matthias Muller. Zoedepth: Zero-shot transfer by combining relative and metric depth. *ArXiv*, abs/2302.12288, 2023. 3
- [6] Guillaume Le Blanc, Youcef Mezouar, and Philippe Martinet. Indoor navigation of a wheeled mobile robot along visual routes. *Proceedings of the 2005 IEEE International*



**1. What is the depth value of the woman?**

Phi2-3B-Spatial: 1247 (GT: 1240)

**2. What is the depth value of the cat?**

Phi2-3B-Spatial: 995 (GT: 987)

**3. Which is closer to the camera, cat or woman?**

Phi2-3B-Spatial: cat corresponds to a depth level of 995, and woman corresponds to a depth level of 1247. Since  $995 < 1247$ , it can be inferred that: cat is closer to the camera, so the answer is: cat. ✓

Phi2-3B: The cat. ✓

QWen1.5-4B: They are equally close. ✗

LLaVA-34B: The woman. ✗

GPT-4o: The woman. ✗

**4. Where is the cat? Answer with the option's letter from the given choices directly.**

- (A) The cat is in the woman's bag.
- (B) The cat is in the woman's pocket.
- (C) The cat is out of the woman's bag.
- (D) The cat is not with the woman.

Phi2-3B-Spatial: (A) ✓

Phi2-3B: (C) ✗

QWen1.5-4B: (C) ✗

LLaVA-34B: (C) ✗

GPT-4o: (A) ✓



**1. What is the depth value of the sign?**

Phi2-3B-Spatial: 4156 (GT: 4137)

**2. What is the depth value of the white car?**

Phi2-3B-Spatial: 28891 (GT: 28479)

**3. Which is closer to the camera, sign or white car?**

Phi2-3B-Spatial: The sign corresponds to a depth measurement of 4153, and the white car corresponds to a depth measurement of 28891. Since  $4153 < 28891$ , it can be inferred that: the sign is closer to the camera. ✓

Phi2-3B: The sign. ✓

QWen1.5-4B: The sign. ✓

LLaVA-34B: The sign. ✓

GPT-4o: The sign. ✓

**4. What is the arrow of sign pointing to? Answer with the option's letter from the given choices directly.**

- (A) The car.
- (B) The grass.
- (C) The sky.
- (D) The building.

Phi2-3B-Spatial: (B) ✓

Phi2-3B: (A) ✗

QWen1.5-4B: (D) ✗

LLaVA-34B: (C) ✗

GPT-4o: (A) ✗

Figure 7. Two conversations in *SpatialBench*. It first asks about depth value of objects, then lets models compare depth between objects. Finally, spatial relationship questions are asked.

- Conference on Robotics and Automation*, pages 3354–3359, 2005. 3
- [7] Boyuan Chen, Zhuo Xu, Sean Kirmani, Brian Ichter, Danny Driess, Pete Florence, Dorsa Sadigh, Leonidas Guibas, and Fei Xia. SpatialVlm: Endowing vision-language models with spatial reasoning capabilities. *ArXiv*, abs/2401.12168, 2024. 3
- [8] Lawrence Yunliang Chen, Simeon Adebola, and Ken Goldberg. Berkeley UR5 demonstration dataset. <https://sites.google.com/view/berkeley-ur5/home>. 3
- [9] Tianheng Cheng, Lin Song, Yixiao Ge, Wenyu Liu, Xinggang Wang, and Ying Shan. Yolo-world: Real-time open-vocabulary object detection. *ArXiv*, abs/2401.17270, 2024. 4
- [10] Wei-Lin Chiang, Zhuohan Li, Zi Lin, Ying Sheng, Zhanghao Wu, Hao Zhang, Lianmin Zheng, Siyuan Zhuang, Yonghao Zhuang, Joseph E Gonzalez, et al. Vicuna: An open-source chatbot impressing gpt-4 with 90%\* chatgpt quality. See <https://vicuna.lmsys.org> (accessed 14 April 2023), 2(3):6, 2023. 3
- [11] Jang Hyun Cho, B. Ivanovic, Yulong Cao, Edward Schmerling, Yue Wang, Xinshuo Weng, Boyi Li, Yurong You, Philipp Krahenbuhl, Yan Wang, and Marco Pavone. Language-image models with 3d understanding. 2024. 3
- [12] Jonathan Crespo, José Carlos Castillo, Óscar Martínez Mozos, and Ramón Barber. Semantic information for robot navigation: A survey. *Applied Sciences*, 2020. 1
- [13] Haoshu Fang, Chenxi Wang, Minghao Gou, and Cewu Lu. Graspnet-1billion: A large-scale benchmark for general object grasping. *2020 IEEE/CVF Conference on Computer Vision and Pattern Recognition (CVPR)*, pages 11441–11450, 2020. 3
- [14] Zhen fei Yin, Jiong Wang, Jianjian Cao, Zhelun Shi, Dingning Liu, Mukai Li, Lu Sheng, Lei Bai, Xiaoshui Huang, Zhiyong Wang, Wanli Ouyang, and Jing Shao. Lamm: Language-assisted multi-modal instruction-tuning dataset, framework, and benchmark. *ArXiv*, abs/2306.06687, 2023. 3
- [15] Yunhai Feng, Nicklas Hansen, Ziyang Xiong, Chandramouli Rajagopalan, and Xiaolong Wang. Finetuning offline world models in the real world. *ArXiv*, abs/2310.16029, 2023. 3
- [16] Wendy Flores-Fuentes, Gabriel Trujillo-Hernández, Iván Y. Alba-Corpus, Julio César Rodríguez-Quiñonez, Jesús E. Mirada-Vega, Daniel Hernández-Balbuena, Fabian Natanael Murrieta-Rico, and Oleg Yu. Sergiyenko. 3d spatial measurement for model reconstruction: A review. *Measurement*, 2022. 1
- [17] Chaoyou Fu, Peixian Chen, Yunhang Shen, Yulei Qin, Mengdan Zhang, Xu Lin, Zhenyu Qiu, Wei Lin, Jinrui Yang, Xiawu Zheng, Ke Li, Xing Sun, and Rongrong Ji. Mme: A comprehensive evaluation benchmark for multimodal large language models. *ArXiv*, abs/2306.13394, 2023. 2, 3, 5, 6, 8
- [18] Huan Fu, Mingming Gong, Chaohui Wang, K. Batmanghelich, and Dacheng Tao. Deep ordinal regression network for monocular depth estimation. *2018 IEEE/CVF Conference on Computer Vision and Pattern Recognition*, pages 2002–2011, 2018. 3
- [19] Jensen Gao, Bidipta Sarkar, Fei Xia, Ted Xiao, Jiajun Wu, Brian Ichter, Anirudha Majumdar, and Dorsa Sadigh. Physically grounded vision-language models for robotic manipulation. *arXiv preprint arXiv:2309.02561*, 2023. 1
- [20] Yash Goyal, Tejas Khot, Douglas Summers-Stay, Dhruv Batra, and Devi Parikh. Making the v in vqa matter: Elevating the role of image understanding in visual question answering. *International Journal of Computer Vision*, 127:398 – 414, 2016. 8
- [21] Jiayuan Gu, Fanbo Xiang, Xuanlin Li, Z. Ling, Xiqiang Liu, Tongzhou Mu, Yihe Tang, Stone Tao, Xinyue Wei, Yuan Yao, Xiao Yuan, Pengwei Xie, Zhiao Huang, Rui Chen, and Hao Su. Maniskill2: A unified benchmark for generalizable manipulation skills. *ArXiv*, abs/2302.04659, 2023. 9
- [22] Faiza Gul, Wan Rahiman, and Syed Sahal Nazli Alhady. A comprehensive study for robot navigation techniques. *Cogent Engineering*, 6, 2019. 3
- [23] Muyang He, Yexin Liu, Boya Wu, Jianhao Yuan, Yuezhe Wang, Tiejun Huang, and Bo Zhao. Efficient multimodal learning from data-centric perspective. *ArXiv*, abs/2402.11530, 2024. 1, 3, 4, 5, 6
- [24] J. Edward Hu, Yelong Shen, Phillip Wallis, Zeyuan Allen-Zhu, Yuanzhi Li, Shean Wang, and Weizhu Chen. Lora: Low-rank adaptation of large language models. *ArXiv*, abs/2106.09685, 2021. 6
- [25] Wen Huang, Hongbin Liu, Minxin Guo, and Neil Zhenqiang Gong. Visual hallucinations of multi-modal large language models. *ArXiv*, abs/2402.14683, 2024. 3
- [26] Drew A. Hudson and Christopher D. Manning. Gqa: A new dataset for real-world visual reasoning and compositional question answering. *2019 IEEE/CVF Conference on Computer Vision and Pattern Recognition (CVPR)*, pages 6693–6702, 2019. 2, 6, 8
- [27] Shahram Izadi, David Kim, Otmar Hilliges, David Molyneaux, Richard A. Newcombe, Pushmeet Kohli, Jamie Shotton, Steve Hodges, Dustin Freeman, Andrew J. Davison, and Andrew William Fitzgibbon. Kinectfusion: real-time 3d reconstruction and interaction using a moving depth camera. *Proceedings of the 24th annual ACM symposium on User interface software and technology*, 2011. 3
- [28] Jitesh Jain, Jianwei Yang, and Humphrey Shi. Vcoder: Versatile vision encoders for multimodal large language models. *ArXiv*, abs/2312.14233, 2023. 3
- [29] Yunfan Jiang, Agrim Gupta, Zichen Zhang, Guanzhi Wang, Yongqiang Dou, Yanjun Chen, Li Fei-Fei, Anima Anandkumar, Yuke Zhu, and Linxi (Jim) Fan. Vima: General robot manipulation with multimodal prompts. *ArXiv*, abs/2210.03094, 2022. 3
- [30] Yizhang Jin, Jian Li, Yexin Liu, Tianjun Gu, Kai Wu, Zhengkai Jiang, Muyang He, Bo Zhao, Xin Tan, Zhenye Gan, Yabiao Wang, Chengjie Wang, and Lizhuang Ma. Efficient multimodal large language models: A survey. *ArXiv*, abs/2405.10739, 2024. 3
- [31] Zhizhong Kang, Juntao Yang, Zhou Yang, and Sai Cheng. A review of techniques for 3d reconstruction of indoor environments. *ISPRS Int. J. Geo Inf.*, 9:330, 2020. 1

- [32] Bing Wen Ke, Anton Obukhov, Shengyu Huang, Nando Metzger, Rodrigo Caye Daudt, and Konrad Schindler. Repurposing diffusion-based image generators for monocular depth estimation. *ArXiv*, abs/2312.02145, 2023. 3
- [33] Alexander Khazatsky, Karl Pertsch, Suraj Nair, Ashwin Balakrishna, Sudeep Dasari, Siddharth Karamcheti, Soroush Nasiriany, Mohan Kumar Srirama, Lawrence Yunliang Chen, Kirsty Ellis, et al. Droid: A large-scale in-the-wild robot manipulation dataset. *arXiv preprint arXiv:2403.12945*, 2024. 3
- [34] Alexander Kirillov, Eric Mintun, Nikhila Ravi, Hanzi Mao, Chloe Rolland, Laura Gustafson, Tete Xiao, Spencer Whitehead, Alexander C. Berg, Wan-Yen Lo, Piotr Dollár, and Ross B. Girshick. Segment anything. *2023 IEEE/CVF International Conference on Computer Vision (ICCV)*, pages 3992–4003, 2023. 4, 5
- [35] Ranjay Krishna, Yuke Zhu, Oliver Groth, Justin Johnson, Kenji Hata, Joshua Kravitz, Stephanie Chen, Yannis Kalantidis, Li-Jia Li, David A. Shamma, Michael S. Bernstein, and Li Fei-Fei. Visual genome: Connecting language and vision using crowdsourced dense image annotations. *International Journal of Computer Vision*, 123:32 – 73, 2016. 2, 4
- [36] Xin Lai, Zhuotao Tian, Yukang Chen, Yanwei Li, Yuhui Yuan, Shu Liu, and Jiaya Jia. Lisa: Reasoning segmentation via large language model. *ArXiv*, abs/2308.00692, 2023. 3
- [37] Edmund Y. Lam. Computational photography with plenoptic camera and light field capture: tutorial. *Journal of the Optical Society of America. A, Optics, image science, and vision*, 32 11:2021–32, 2015. 1
- [38] Sergey Levine and Dhruv Shah. Learning robotic navigation from experience: principles, methods and recent results. *Philosophical Transactions of the Royal Society B*, 378, 2022. 1
- [39] Bohao Li, Rui Wang, Guangzhi Wang, Yuying Ge, Yixiao Ge, and Ying Shan. Seed-bench: Benchmarking multimodal llms with generative comprehension. *ArXiv*, abs/2307.16125, 2023. 3, 8
- [40] Junnan Li, Dongxu Li, Silvio Savarese, and Steven C. H. Hoi. Blip-2: Bootstrapping language-image pre-training with frozen image encoders and large language models. In *International Conference on Machine Learning*, 2023. 1
- [41] Jianing Li, Xi Nan, Ming Lu, Li Du, and Shanghang Zhang. Proximity qa: Unleashing the power of multi-modal large language models for spatial proximity analysis. *ArXiv*, abs/2401.17862, 2024. 3, 4
- [42] Xiaoqi Li, Mingxu Zhang, Yiran Geng, Haoran Geng, Yuxing Long, Yan Shen, Renrui Zhang, Jiaming Liu, and Hao Dong. Manipllm: Embodied multimodal large language model for object-centric robotic manipulation. In *Proceedings of the IEEE/CVF Conference on Computer Vision and Pattern Recognition (CVPR)*, pages 18061–18070, 2024. 1
- [43] Yifan Li, Yifan Du, Kun Zhou, Jinpeng Wang, Wayne Xin Zhao, and Ji rong Wen. Evaluating object hallucination in large vision-language models. In *Conference on Empirical Methods in Natural Language Processing*, 2023. 8
- [44] Yanwei Li, Yuechen Zhang, Chengyao Wang, Zhisheng Zhong, Yixin Chen, Ruihang Chu, Shaoteng Liu, and Jiaya Jia. Mini-gemini: Mining the potential of multi-modality vision language models. *ArXiv*, abs/2403.18814, 2024. 3
- [45] Tsung-Yi Lin, Michael Maire, Serge J. Belongie, James Hays, Pietro Perona, Deva Ramanan, Piotr Dollár, and C. Lawrence Zitnick. Microsoft coco: Common objects in context. In *European Conference on Computer Vision*, 2014. 2, 4
- [46] Haotian Liu, Chunyuan Li, Qingyang Wu, and Yong Jae Lee. Visual instruction tuning. *ArXiv*, abs/2304.08485, 2023. 1, 3, 5, 6
- [47] Shilong Liu, Zhaoyang Zeng, Tianhe Ren, Feng Li, Hao Zhang, Jie Yang, Chun yue Li, Jianwei Yang, Hang Su, Jun-Juan Zhu, and Lei Zhang. Grounding dino: Marrying dino with grounded pre-training for open-set object detection. *ArXiv*, abs/2303.05499, 2023. 4
- [48] Yuanzhan Liu, Haodong Duan, Yuanhan Zhang, Bo Li, Songyang Zhang, Wangbo Zhao, Yike Yuan, Jiaqi Wang, Conghui He, Ziwei Liu, Kai Chen, and Dahua Lin. Mm-bench: Is your multi-modal model an all-around player? *ArXiv*, abs/2307.06281, 2023. 3, 8
- [49] Brandon McKinzie, Zhe Gan, Jean-Philippe Fauconnier, Sam Dodge, Bowen Zhang, Philipp Dufter, Dhruvi Shah, Xianzhi Du, Futang Peng, Floris Weers, et al. Mm1: Methods, analysis & insights from multimodal llm pre-training. *arXiv preprint arXiv:2403.09611*, 2024. 3
- [50] Abhishek Padalkar, Acorn Pooley, Ajinkya Jain, Alex Bewley, Alex Herzog, Alex Irpan, Alexander Khazatsky, Anant Rai, Anikait Singh, Anthony Brohan, et al. Open x-embodiment: Robotic learning datasets and rt-x models. *arXiv preprint arXiv:2310.08864*, 2023. 1, 2, 3, 4, 6
- [51] Hailong Pan, Tao Guan, Yawei Luo, Liya Duan, Yuan Tian, Liu Yi, Yizhu Zhao, and Junqing Yu. Dense 3d reconstruction combining depth and rgb information. *Neurocomputing*, 175:644–651, 2016. 3
- [52] Xingang Pan, Jianping Shi, Ping Luo, Xiaogang Wang, and Xiaoou Tang. Spatial as deep: Spatial cnn for traffic scene understanding. In *AAAI Conference on Artificial Intelligence*, 2017. 1
- [53] Alec Radford, Jong Wook Kim, Chris Hallacy, Aditya Ramesh, Gabriel Goh, Sandhini Agarwal, Girish Sastry, Amanda Askell, Pamela Mishkin, Jack Clark, Gretchen Krueger, and Ilya Sutskever. Learning transferable visual models from natural language supervision. In *International Conference on Machine Learning*, 2021. 6, 9
- [54] René Ranftl, Katrin Lasinger, David Hafner, Konrad Schindler, and Vladlen Koltun. Towards robust monocular depth estimation: Mixing datasets for zero-shot cross-dataset transfer. *IEEE Transactions on Pattern Analysis and Machine Intelligence*, 44:1623–1637, 2019. 3, 4
- [55] Tianhe Ren, Shilong Liu, Ailing Zeng, Jing Lin, Kunchang Li, He Cao, Jiayu Chen, Xinyu Huang, Yukang Chen, Feng Yan, Zhaoyang Zeng, Hao Zhang, Feng Li, Jie Yang, Hongyang Li, Qing Jiang, and Lei Zhang. Grounded sam: Assembling open-world models for diverse visual tasks. *ArXiv*, abs/2401.14159, 2024. 4
- [56] Christoph Schuhmann, Romain Beaumont, Richard Vencu, Cade Gordon, Ross Wightman, Mehdi Cherti, Theo

- Coombes, Aarush Katta, Clayton Mullis, Mitchell Wortsman, Patrick Schramowski, Srivatsa Kundurthy, Katherine Crowson, Ludwig Schmidt, Robert Kaczmarczyk, and Jenia Jitsev. Laion-5b: An open large-scale dataset for training next generation image-text models. *ArXiv*, abs/2210.08402, 2022. 6
- [57] Haochen Shi, Huazhe Xu, Samuel Clarke, Yunzhu Li, and Jiajun Wu. Robocook: Long-horizon elasto-plastic object manipulation with diverse tools. *ArXiv*, abs/2306.14447, 2023. 3
- [58] Mohit Shridhar, Lucas Manuelli, and Dieter Fox. Cliport: What and where pathways for robotic manipulation. *ArXiv*, abs/2109.12098, 2021. 1
- [59] Gemini Team, Rohan Anil, Sebastian Borgeaud, Yonghui Wu, Jean-Baptiste Alayrac, Jiahui Yu, Radu Soricut, Johan Schalkwyk, Andrew M Dai, Anja Hauth, et al. Gemini: a family of highly capable multimodal models. *arXiv preprint arXiv:2312.11805*, 2023. 1, 5
- [60] Hugo Touvron, Thibaut Lavril, Gautier Izacard, Xavier Martinet, Marie-Anne Lachaux, Timothée Lacroix, Baptiste Rozière, Naman Goyal, Eric Hambro, Faisal Azhar, Aurelien Rodriguez, Armand Joulin, Edouard Grave, and Guillaume Lample. Llama: Open and efficient foundation language models. *ArXiv*, abs/2302.13971, 2023. 3, 6
- [61] Homer Walke, Kevin Black, Abraham Lee, Moo Jin Kim, Maximilian Du, Chongyi Zheng, Tony Zhao, Philippe Hansen-Estruch, Quan Ho Vuong, Andre Wang He, Vivek Myers, Kuan Fang, Chelsea Finn, and Sergey Levine. Bridgedata v2: A dataset for robot learning at scale. In *Conference on Robot Learning*, 2023. 3
- [62] Yixuan Wang, Zhuoran Li, Mingtong Zhang, K. Driggs-Campbell, Jiajun Wu, Li Fei-Fei, and Yunzhu Li. D3fields: Dynamic 3d descriptor fields for zero-shot generalizable robotic manipulation. *ArXiv*, abs/2309.16118, 2023. 3
- [63] Steffen Werner, Bernd Krieg-Brückner, Hanspeter A. Mallot, Karin Schweizer, and Christian Freksa. Spatial cognition: The role of landmark, route, and survey knowledge in human and robot navigation. In *GI Jahrestagung*, 1997. 1
- [64] Zhixuan Xu, Chongkai Gao, Zixuan Liu, Gang Yang, Chenrui Tie, Haozhuo Zheng, Haoyu Zhou, Weikun Peng, Debang Wang, Tianyi Chen, Zhouliang Yu, and Lin Shao. Mani-foundation model for general-purpose robotic manipulation of contact synthesis with arbitrary objects and robots. 2024. 3
- [65] Jihan Yang, Runyu Ding, Ellis L Brown, Xiaojuan Qi, and Saining Xie. V-irl: Grounding virtual intelligence in real life. *ArXiv*, abs/2402.03310, 2024. 3
- [66] Lihe Yang, Bingyi Kang, Zilong Huang, Xiaogang Xu, Jia-ashi Feng, and Hengshuang Zhao. Depth anything: Unleashing the power of large-scale unlabeled data. *ArXiv*, abs/2401.10891, 2024. 3
- [67] Zhengyuan Yang, Linjie Li, Kevin Lin, Jianfeng Wang, Chung-Ching Lin, Zicheng Liu, and Lijuan Wang. The dawn of lmms: Preliminary explorations with gpt-4v(ision). *ArXiv*, abs/2309.17421, 2023. 1, 2, 5
- [68] Haoxuan You, Haotian Zhang, Zhe Gan, Xianzhi Du, Bowen Zhang, Zirui Wang, Liangliang Cao, Shih-Fu Chang, and Yinfei Yang. Ferret: Refer and ground anything anywhere at any granularity. *ArXiv*, abs/2310.07704, 2023. 3
- [69] Alex Young, Bei Chen, Chao Li, Chengen Huang, Ge Zhang, Guanwei Zhang, Heng Li, Jiangcheng Zhu, Jianqun Chen, Jing Chang, et al. Yi: Open foundation models by 01. ai. *arXiv preprint arXiv:2403.04652*, 2024. 3
- [70] Jianhao Yuan, Shuyang Sun, Daniel Omeiza, Bo Zhao, Paul Newman, Lars Kunze, and Matthew Gadd. Rag-driver: Generalisable driving explanations with retrieval-augmented in-context learning in multi-modal large language model. *arXiv preprint arXiv:2402.10828*, 2024. 1
- [71] Yuqian Yuan, Wentong Li, Jian Liu, Dongqi Tang, Xinjie Luo, Chi Qin, Lei Zhang, and Jianke Zhu. Osprey: Pixel understanding with visual instruction tuning. *ArXiv*, abs/2312.10032, 2023. 3
- [72] Xiang Yue, Yuansheng Ni, Kai Zhang, Tianyu Zheng, Ruoqi Liu, Ge Zhang, Samuel Stevens, Dongfu Jiang, Weiming Ren, Yuxuan Sun, Cong Wei, Botao Yu, Ruibin Yuan, Renliang Sun, Ming Yin, Boyuan Zheng, Zhenzhu Yang, Yibo Liu, Wenhao Huang, Huan Sun, Yu Su, and Wenhua Chen. Mmmu: A massive multi-discipline multimodal understanding and reasoning benchmark for expert agi. *ArXiv*, abs/2311.16502, 2023. 3
- [73] Xiaohua Zhai, Basil Mustafa, Alexander Kolesnikov, and Lucas Beyer. Sigmoid loss for language image pre-training. *2023 IEEE/CVF International Conference on Computer Vision (ICCV)*, pages 11941–11952, 2023. 6
- [74] Ao Zhang, Wei Ji, and Tat-Seng Chua. Next-chat: An lmm for chat, detection and segmentation. *ArXiv*, abs/2311.04498, 2023. 3
- [75] Hao Zhang, Hongyang Li, Feng Li, Tianhe Ren, Xueyan Zou, Shilong Liu, Shijia Huang, Jianfeng Gao, Lei Zhang, Chun yue Li, and Jianwei Yang. Llava-grounding: Grounded visual chat with large multimodal models. *ArXiv*, abs/2312.02949, 2023. 3
- [76] Bo Zhao, Boya Wu, Muiyang He, and Tiejun Huang. Svit: Scaling up visual instruction tuning. *arXiv preprint arXiv:2307.04087*, 2023. 3, 4
- [77] Xueyan Zou, Jianwei Yang, Hao Zhang, Feng Li, Linjie Li, Jianfeng Gao, and Yong Jae Lee. Segment everything everywhere all at once. *ArXiv*, abs/2304.06718, 2023. 4